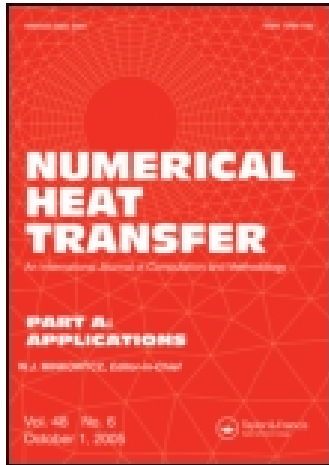


This article was downloaded by: [Thammasat University Libraries]

On: 28 April 2015, At: 19:40

Publisher: Taylor & Francis

Informa Ltd Registered in England and Wales Registered Number: 1072954 Registered office: Mortimer House, 37-41 Mortimer Street, London W1T 3JH, UK



## Numerical Heat Transfer, Part A: Applications: An International Journal of Computation and Methodology

Publication details, including instructions for authors and subscription information:

<http://www.tandfonline.com/loi/unht20>

### Heat Transfer Analysis of the Human Eye During Exposure to Sauna Therapy

Teerapot Wessapan<sup>a</sup> & Phadungsak Rattanadecho<sup>b</sup>

<sup>a</sup> School of Aviation, Eastern Asia University, Pathumthani, Thailand

<sup>b</sup> Department of Mechanical Engineering, Faculty of Engineering, Thammasat University (Rangsit Campus), Center of Excellence in Electromagnetic Energy Utilization in Engineering (CEEE), Pathumthani, Thailand

Published online: 23 Apr 2015.



[Click for updates](#)

To cite this article: Teerapot Wessapan & Phadungsak Rattanadecho (2015) Heat Transfer Analysis of the Human Eye During Exposure to Sauna Therapy, Numerical Heat Transfer, Part A: Applications: An International Journal of Computation and Methodology, 68:5, 566-582, DOI: [10.1080/10407782.2014.986393](https://doi.org/10.1080/10407782.2014.986393)

To link to this article: <http://dx.doi.org/10.1080/10407782.2014.986393>

PLEASE SCROLL DOWN FOR ARTICLE

Taylor & Francis makes every effort to ensure the accuracy of all the information (the "Content") contained in the publications on our platform. However, Taylor & Francis, our agents, and our licensors make no representations or warranties whatsoever as to the accuracy, completeness, or suitability for any purpose of the Content. Any opinions and views expressed in this publication are the opinions and views of the authors, and are not the views of or endorsed by Taylor & Francis. The accuracy of the Content should not be relied upon and should be independently verified with primary sources of information. Taylor and Francis shall not be liable for any losses, actions, claims, proceedings, demands, costs, expenses, damages, and other liabilities whatsoever or howsoever caused arising directly or indirectly in connection with, in relation to or arising out of the use of the Content.

This article may be used for research, teaching, and private study purposes. Any substantial or systematic reproduction, redistribution, reselling, loan, sub-licensing, systematic supply, or distribution in any form to anyone is expressly forbidden. Terms &

Conditions of access and use can be found at <http://www.tandfonline.com/page/terms-and-conditions>

## HEAT TRANSFER ANALYSIS OF THE HUMAN EYE DURING EXPOSURE TO SAUNA THERAPY

Teerapot Wessapan<sup>1</sup> and Phadungsak Rattanadecho<sup>2</sup>

<sup>1</sup>School of Aviation, Eastern Asia University, Pathumthani, Thailand

<sup>2</sup>Department of Mechanical Engineering, Faculty of Engineering, Thammasat University (Rangsit Campus), Center of Excellence in Electromagnetic Energy Utilization in Engineering (CEEE), Pathumthani, Thailand

*Among the reported health benefits of a sauna session are weight loss, detoxification of the body, and improved blood circulation. Side effects of sauna therapy, both beneficial and detrimental, also exist. It is well known that the human eye is one of the most sensitive parts of the entire human body when exposed to high ambient temperature and humidity levels such as in sauna therapy. This sauna heat interacts with the human eye and may lead to a variety of ocular effects due to radiation emitted by the heater and high ambient temperature. However, the resulting thermophysiological response of the human eye to various exposure conditions during sauna therapy is not well understood. Therefore, it is of interest to investigate the potential ocular effects that may occur during sauna exposure. This study presents a numerical analysis of heat transfer in a heterogeneous model of a human eye exposed to sauna. The heat transfer model is developed based on porous media theories. In the heterogeneous human eye model, the effects of room air temperature and heater temperature on the intraocular temperature increase are systematically investigated. The study intends to focus attention on the different heat transfer characteristics between conventional sauna (mainly convection) and infrared sauna (mainly radiation). The results show that at the same room air temperature, the circulatory patterns within the anterior chamber of the eye in regard to infrared sauna are more rapid than those for the conventional sauna. Moreover, eye temperature is also higher in the infrared sauna than in the conventional sauna. The maximum temperatures of the eye exposed to conventional and infrared saunas at room air temperature of 80°C are 48.25°C and 52.90°C, respectively. From the values obtained, a guideline can be recommended to indicate the limitations in regard to temperature increase in the human eye due to sauna therapy.*

### 1. INTRODUCTION

A sauna is a small room designed to be heated to very high temperatures with well-controlled humidity. Sauna therapy has been used for hundreds of years as a standard health-promoting practice, and can also be part of an effective weight loss program. Saunas can be divided into two basic types: conventional saunas that warm

Received 2 July 2014; accepted 7 November 2014.

Address correspondence to Phadungsak Rattanadecho, Department of Mechanical Engineering, Faculty of Engineering, Thammasat University (Rangsit Campus), Center of Excellence in Electromagnetic Energy Utilization in Engineering (CEEE), Pathumthani, 12120, Thailand. E-mail: ratphadu@engr.tu.ac.th

Color versions of one or more of the figures in the article can be found online at [www.tandfonline.com/unht](http://www.tandfonline.com/unht).

## NOMENCLATURE

$C$	specific heat capacity (J/(kg K))	$\beta$	volume expansion coefficient (1/K)
$e$	tear evaporation heat loss (W/m <sup>2</sup> )	$\varepsilon$	porosity
$F$	view factor	$\rho$	density (kg/m <sup>3</sup> )
$G$	irradiation (W/m <sup>2</sup> )	$\sigma$	Stefan-Boltzmann constant
$h$	convection coefficient (W/m <sup>2</sup> K)	$\omega_b$	blood perfusion rate (1/s)
$k$	thermal conductivity (W/(m K))	$\Gamma$	external surface area
$n$	normal vector	<b>Subscripts</b>	
$p$	pressure (N/m <sup>2</sup> )	am	ambient
$Q$	heat source (W/m <sup>3</sup> )	b	blood
$T$	temperature (K)	ext	external
$t$	time	$i$	subdomain
$u$	velocity (m/s)	met	metabolic

the air and infrared saunas that warm objects (Figure 1). The conventional sauna relies on indirect means of heat: the air is heated and then the hot air makes contact with the user's skin (convection and conduction). In the infrared sauna, the radiant infrared energy heats the air only slightly while heating the user's body directly (radiation). However, side effects of sauna therapy, both beneficial and detrimental, exist.

Increases in the human eye temperature are important for both laboratory and clinical investigations [1]. Environmental conditions, namely ambient temperature, influence the temperature increase in the eye. It is well known that the eye is one of the organs most sensitive to environmental factors such as extreme temperature conditions. This is due to the fact that the crystalline lens and cornea are nonvascular tissues with a low metabolism, and also that the eye has no thermal sensors or protective reflexes. The severity of the physiological effect produced by small temperature increases can cause deterioration in eyesight. There are medical case reports on the formation of cataracts in humans following accidental exposure to radiation [2]. In fact, a small temperature increase in the eye of 3–5°C can induce the formation

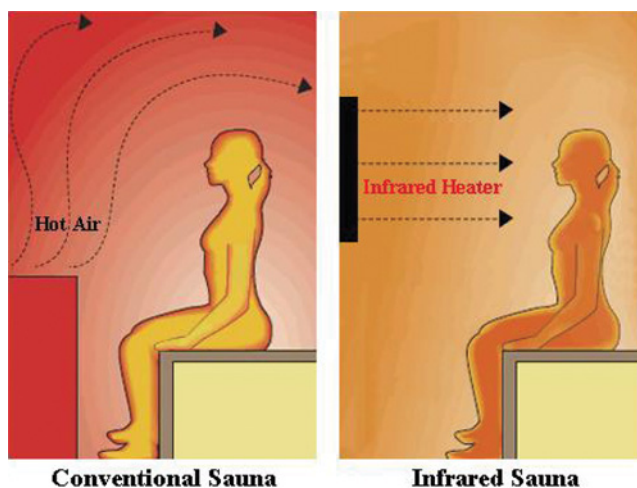


Figure 1. Conventional and infrared saunas.

of cataracts [3]. Additionally, it is reported that a temperature above 41°C is necessary for the production of posterior lens opacity [4]. However, the resulting thermophysiological response of the human eye to sauna exposure is not well understood. In order to gain insight into the phenomena occurring within the human eye with temperature distribution induced by sauna use, a detailed knowledge of both absorbed radiation and temperature distribution is necessary. Thus, it is of interest to investigate the potential ocular effects that occur during exposure to sauna.

The thermal modeling of human tissue is important as a tool to investigate the effect of external heat sources and to predict abnormalities in the tissue. Most early studies on heat transfer analysis in human tissue, especially in the eye, used heat conduction equations [5–11]. Some studies were carried out on natural convection in the eye based on heat conduction models [12, 13]. Ooi and Ng [13, 14] studied the effect of aqueous humor (AH) hydrodynamics on heat transfer in the eye based on a heat conduction model. Meanwhile, the bioheat equation introduced by Pennes [15, 16], based on the heat diffusion equation for a blood-perfused tissue, is also used for modeling heat transfer in the eye [17, 18]. Ooi and Ng also developed a three-dimensional (3D) model of the eye [19], extending their 2D model [18]. Porous media models have recently been utilized to investigate the transport phenomena in biological media rather than a simplified bioheat model [20–22]. Shafahi and Vafai [23] proposed porous media along with a natural convection model to analyze ocular thermal characteristics during exposure to thermal disturbances. Other research groups conducted numerical analyses of heat and electromagnetic (EM) dissipation in the eye [24–32]. Ooi et al. conducted advanced numerical modeling of the human eye based on the boundary element method [33–37].

Our research group has numerically investigated the temperature increase in human tissue subjected to EM fields in regard to many problems [37–45]. Wessapan et al. [38, 39] utilized a 2D finite-element method (FEM) to determine the specific absorption rate (SAR) and temperature increase in the human body exposed to leaking EM waves. Wessapan et al. [40, 41] developed a 3D model of the human head in order to investigate the SAR and temperature distributions in the human head during exposure to cellphone radiation. Keangin et al. [42–44] carried out a numerical simulation of liver cancer treatment using a complete mathematical model that considered the coupled model of EM wave propagation, heat transfer, and mechanical deformation in the biological tissue in the couple's way (two or more equations are being solved simultaneously). Wessapan et al. [45–47] investigated the SAR and temperature distribution in the eye during exposure to EM waves using the porous media theory.

Advanced models of the eye based on porous media and natural convection theory have been used in various heat transfer problems [29–36, 45–47]. However, most studies have mainly focused on the effects of convective boundary conditions and have not considered the effects of radiation from high-temperature sources in the simulations. In sauna therapy, these radiation effects result in greater heat transfer toward the eye, which can cause injury to the eye. Therefore, in order to provide adequate information on the levels of exposure and health effects from sauna therapy, it is essential to consider the combined effects of radiation and convection from sauna exposure in the analysis.

This study presents a simulation of the temperature distribution in an anatomical human eye exposed to sauna under various conditions. The temperature

distribution in various tissues in the eye during exposure is obtained by numerical simulation of a heat transfer model that is then developed based on porous media theories. This study intends to focus attention on the differences in heat transfer characteristics between conventional sauna (mainly convection) and infrared sauna (mainly radiation). A 2D heterogeneous human eye model is used to simulate temperature distribution and fluid flow in the eye model. The analysis of heat transfer in the eye is investigated using a heat transfer model (based on porous media theory) which was first proposed by Shafahi and Vafai [23]. In the heterogeneous eye model, the effects of room air temperature and heater temperature on temperature distribution and fluid flow in the eye during exposure to sauna are systematically investigated. Temperature distribution and fluid flow obtained by numerical simulation of heat transfer equations based on porous media theory are presented. In this work, the model excluded the presence of both eyelid and metabolic heat generation in order to simplify the modeling procedures. The obtained values represent the phenomena accurately in determining temperature increase and fluid flow in the eye, as well as indicating the limitations that must be considered when temperature increases due to sauna exposure under different conditions.

## 2. FORMULATION OF THE PROBLEM

In many countries, sauna has always been a part of daily life. However, side effects of sauna therapy, both beneficial and detrimental, exist. Figure 2 shows the eye exposed to sauna under various conditions. The sauna heats the eye primarily by conduction and convection from the heated air and by radiation from the heated surfaces in the sauna room, which leads to tissue damage and cataract formation. Due to ethical considerations, exposure of humans to sauna for experimental purposes is limited; Therefore, it is more convenient to develop a realistic human eye model through numerical simulation. Analysis of the heat transfer in the eye will be illustrated in Section 3. The system of governing equations and the boundary conditions is solved numerically using the FEM.

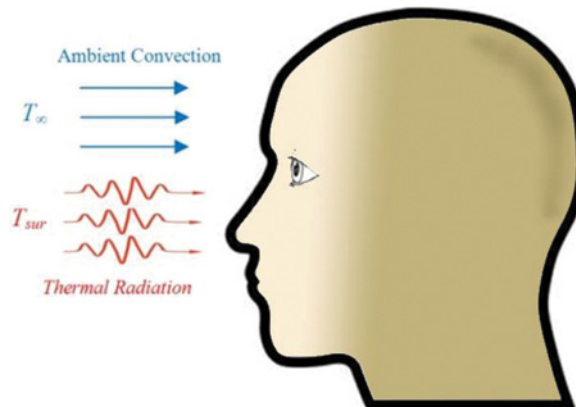


Figure 2. Human eye exposed to sauna therapy.

### 3. METHODS AND MODEL

The first step in evaluating the effects of exposure to sauna therapy is to determine the energy transferred by convection, radiation, and the evaporation process as well as its spatial distribution. Thereafter, energy absorption which results in a temperature increase in the eye and other processes of transport phenomena can be considered.

#### 3.1. Physical Model

In this study, a 2D model of the eye, which follows the physical model in the previous research [23], is developed. Figure 3 shows the 2D eye model used in this study. This model comprises seven types of tissue: cornea, anterior chamber, posterior chamber, iris, sclera, lens, and vitreous. These tissues have different dielectric and thermal properties. In the scleral layer, there are two further layers known as the choroid and retina, which are relatively thin compared with the sclera. To simplify the problem, these layers are assumed to be homogeneous. The iris and sclera, which have the same properties, are modeled together as one homogenous region [13]. The thermal properties of these tissues are given in Table 1. Each tissue is assumed to be homogeneous and thermally isotropic.

#### 3.2. Equations for Heat Transfer and Flow Analysis

To solve the thermal problem, a model of both unsteady heat transfer and boundary conditions is investigated. Heat transfer analysis of the eye is modeled in two dimensions. To simplify the problem, the following assumptions are made:

1. Human tissue is a biomaterial with constant thermal properties.
2. There is no phase change of substance in the tissue.

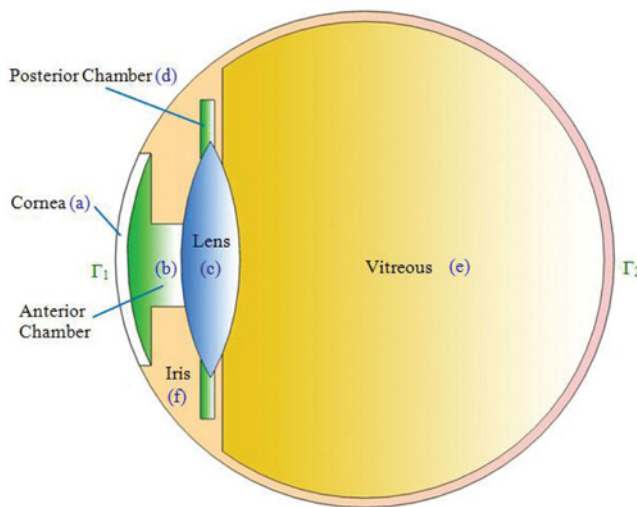


Figure 3. Vertical cross section of the human eye [23].

**Table 1.** Thermal properties of the eye [13]

Tissue	$\rho$ (kg/m <sup>3</sup> )	$k$ (W/m <sup>2</sup> C)	$C_p$ (J/kg <sup>o</sup> C)	$\mu$ (N s/m <sup>2</sup> )	$\beta$ (1/K)
Cornea ( <i>a</i> )	1,050	0.58	4,178	—	—
Anterior chamber ( <i>b</i> )	996	0.58	3,997	0.00074	0.000337
Lens ( <i>c</i> )	1,000	0.4	3,000	—	—
Posterior chamber ( <i>d</i> )	996	0.58	3,997	—	—
Vitreous ( <i>e</i> )	1,100	0.603	4,178	—	—
Sclera ( <i>f</i> )	1,050	1.0042	3,180	—	—
Iris ( <i>f</i> )	1,050	1.0042	3,180	—	—

3. There is a local thermal equilibrium between blood and tissue.
4. There is no chemical reaction in the tissue.

This study utilized a pertinent thermal model based according to porous media theory [23] to investigate the heat transfer behavior of the eye when exposed to sauna.

In this study, the motion of fluid is considered only inside the anterior chamber [13]. There is blood flow in the iris/sclera, which plays the role of adjusting eye temperature to the rest of the body [23]. For the remaining parts of the eye, metabolic heat generation is ignored based on the fact that these comprise mainly water [13]. The equation governing the flow of heat in the cornea, posterior chamber, lens, and vitreous resembles the classical heat conduction equation given by Eq. (1):

$$\rho_i C_i \frac{\partial T_i}{\partial t} = \nabla \cdot (k_i \nabla T_i) \quad ; i = a, c, d, e \quad (1)$$

This model accounts for the existence of AH in the anterior chamber. The heat transfer process consists of both conduction and natural convection, which can be written as follows:

Continuity equation:

$$\nabla \cdot u_i = 0; \quad i = b \quad (2)$$

Momentum equation:

$$\begin{aligned} \rho_i \frac{\partial u_i}{\partial t} + \rho_i u_i \nabla \cdot u_i = -\nabla p_i + \nabla \cdot [\mu(\nabla u_i + \nabla u_i^T)] \\ + \rho_i g \beta_i (T_i - T_{\text{ref}}); \quad i = b \end{aligned} \quad (3)$$

where  $i$  denotes each subdomain in the eye model as shown in Figure 3,  $\rho$  is the tissue density (kg/m<sup>3</sup>),  $\beta$  is the volume expansion coefficient (1/K),  $u$  is the velocity (m/s),  $p$  is the pressure (N/m<sup>2</sup>),  $\mu$  is the dynamic viscosity of AH (N s/m<sup>2</sup>),  $t$  is time,  $T$  is the tissue temperature (K), and  $T_{\text{ref}}$  is the reference temperature considered here, which is 37°C. The effects of buoyancy due to temperature gradient are modeled using the Boussinesq approximation, which states that the density of a given fluid changes slightly with temperature but negligibly with pressure [13].

Energy equation:

$$\rho_i C_i \frac{\partial T_i}{\partial t} - \nabla \cdot (k_i \nabla T_i) = -\rho C_i u_i \cdot \nabla T_i; \quad i = b \quad (4)$$

The sclera/iris is modeled as a porous medium with blood perfusion, which assumes that local thermal equilibrium exists between blood and tissue. The blood perfusion rate used is 0.004 1/s. A modified Pennes' bioheat equation [20, 23] is used to calculate temperature distribution in the sclera/iris:

$$(1 - \varepsilon) \rho_i C_i \frac{\partial T_i}{\partial t} = \nabla \cdot ((1 - \varepsilon) k_i \nabla T_i) + \rho_b C_b \omega_b (T_b - T_i)_{\text{ext}}; \quad i = f \quad (5)$$

where  $C$  is the heat capacity of tissue (J/kg K),  $k$  is the thermal conductivity of tissue (W/m K),  $T_b$  is the temperature of blood (K),  $\rho_b$  is the density of blood (kg/m<sup>3</sup>),  $C_b$  is the specific heat capacity of blood (J/kg K), and  $\omega_b$  is the blood perfusion rate (1/s).

In the analysis, the porosity ( $\varepsilon$ ) used is assumed to be 0.6. Heat conduction between tissue and blood flow is approximated by the blood perfusion term,  $\rho_b C_b \omega_b (T_b - T)$ .

### 3.3. Boundary Condition for Heat Transfer Analysis

The corneal surface, shown in Figure 4, is considered under convective, radiative, and evaporative boundary conditions. The study focuses on the variation in heat transfer characteristics between a conventional sauna (surface-to-ambient radiation) and an infrared sauna (surface-to-surface radiation).

**3.3.1. Conventional sauna (Case I).** In this case, the room air temperature is assumed to be equal to the room surface temperature (walls). Therefore, it is reasonable to simplify the radiation at the corneal surface as a surface-to-ambient radiation type:

$$-n \cdot (-k \nabla T) = h_{\text{am}} (T_i - T_{\text{am}}) + \varepsilon \sigma (T_i^4 - T_{\text{am}}^4) + e \quad \text{on } \Gamma_1 \quad i = a \quad (6)$$

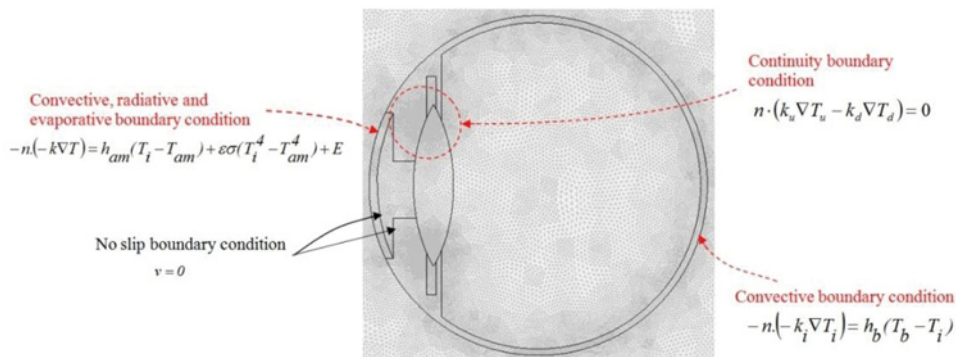


**Figure 4.** A 2D finite-element mesh of the eye model and boundary conditions for analysis.

**3.3.2. Infrared sauna (Case II).** In this case, the infrared heater is at a temperature higher than that of the walls, while the room air temperature is assumed to be equal to the wall temperature. Radiation at the corneal surface is a multiple surface radiation exchange, and thus surface-to-surface radiation is modeled using view factor analysis:

$$-n \cdot (-k \nabla T) = h_{\text{am}}(T_i - T_{\text{am}}) + \varepsilon(G - \sigma T_i^4) + e \quad \text{on } \Gamma_1 \quad i = a \quad (7)$$

Irradiation,  $G$ , can be written as a sum according to

$$G = F_{\text{heater}} \sigma T_{\text{heater}}^4 + F_{\text{am}} \sigma T_{\text{am}}^4 + e \quad (8)$$

where  $\Gamma_i$  is the external surface area corresponding to section  $i$ ,  $e$  is the tear evaporation heat loss ( $\text{W}/\text{m}^2$ ),  $T_{\text{am}}$  is the ambient temperature (K),  $h_{\text{am}}$  is the convection coefficient ( $\text{W}/\text{m}^2 \text{K}$ ),  $F$  is the view factor between surfaces,  $F_{\text{heater}}$  is the heater view factor, and  $F_{\text{am}}$  is the ambient view factor.

The temperature of blood is generally assumed to be the same as the body core temperature, which causes heat to be transferred to the eye [13]. The surface of the sclera is assumed to be under the convective boundary condition:

$$-n \cdot (-k_i \nabla T_i) = h_b(T_b - T_i) \quad \text{on } \Gamma_2 \quad i = f \quad (9)$$

where  $h_b$  is the convection coefficient of blood ( $65 \text{ W}/\text{m}^2 \text{K}$ ), and  $\Gamma_1$  and  $\Gamma_2$  are the corneal and scleral surfaces of the eye, respectively.

### 3.4. Calculation Procedure

In this study, FEM is used to analyze the transient problems. In order to obtain a good approximation, a fine mesh is specified in the sensitive areas. This study provides a variable mesh method for solving the problem, as shown in Figure 4. The system of governing equations and boundary conditions is then solved. All computational processes are implemented using COMSOL<sup>TM</sup> Multiphysics to demonstrate the phenomenon that occurs in the eye exposed to sauna.

The 2D model is discretized using triangular elements, and the Lagrange quadratic is then used to approximate the temperature variation across each element. A convergence test is carried out to identify the number of elements required. This convergence test leads to a grid with approximately 10,000 elements. It is reasonable to assume that, at this element number, the accuracy of the simulation results is independent of the number of elements.

## 4. RESULTS AND DISCUSSION

In this analysis, the effects of room air temperature and heater temperature on temperature distribution and fluid flow in the eye during exposure to sauna are systematically investigated. The following discussion focuses on the transport phenomena that occur within the eye exposed to conventional and infrared sauna.

In this study, the effect of thermoregulation mechanisms has been ignored. The convective coefficient due to the blood flow inside the sclera is set to  $65 \text{ W/m}^2 \text{ K}$  [13]. For the simulation, the thermal properties are taken directly from Table 1.

#### 4.1. Verification of the Model

In order to verify the accuracy of the present numerical model, the simple cases of the simulated results from this study are validated against the numerical results obtained with the same geometric model by Shafahi and Vafai [23]. Moreover, the numerical results are then compared to the experimental results from a rabbit study by Legendijk [5]. The validation case assumes that the rabbit body temperature was  $38.8^\circ\text{C}$ , the tear evaporation heat loss is  $40 \text{ W/m}^2$ , the ambient temperature is  $25^\circ\text{C}$ , and the convection coefficient of ambient air is  $20 \text{ W/m}^2 \text{ K}$ . The results of the selected test case are shown in Figure 5 for ocular temperature distribution. Figure 5 clearly shows a good agreement for ocular temperature distribution between the present solution and those of Shafahi and Vafai [23] and Legendijk [5]. This favorable comparison lends confidence to the accuracy of the present numerical model.

#### 4.2. Conventional Sauna (Case I)

**4.2.1. Effect of room air temperature.** *In the case of the conventional sauna, when the room air temperature is higher than the eye temperature, namely 60, 80,*

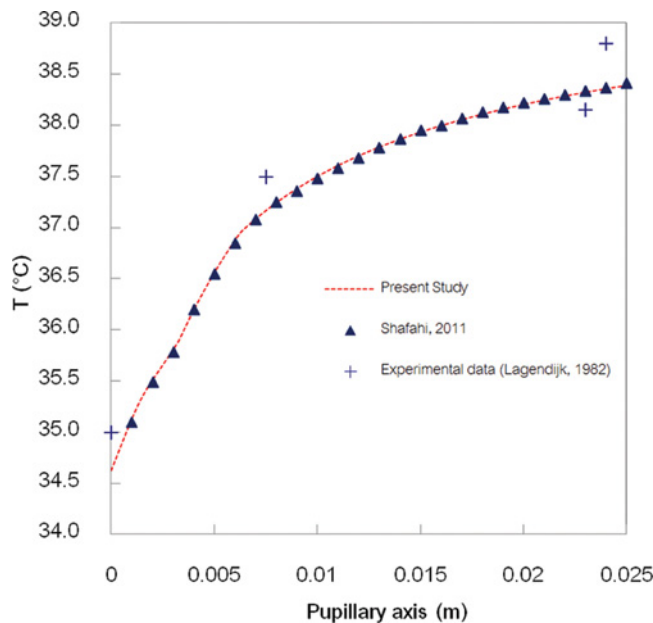


**Figure 5.** Comparison of the calculated temperature distribution to temperature distribution obtained by Shafahi and Vafai [23] and Legendijk's experimental data [5];  $h_{\text{am}} = 20 \text{ W/m}^2 \text{ K}$  and  $T_{\text{am}} = 25^\circ\text{C}$ .

and 100°C (shown in Figure 6), heat convected and radiated from the ambient air flows into the eye and the ocular temperature rises above normal body temperature. At  $t=10$  min, the maximum temperatures inside the eye are 42.91, 48.25, and 53.81°C for room air temperatures of 60, 80, and 100°C, respectively.

### 4.3. Infrared Sauna (Case II)

This case assumes that the heater view factor ( $F_{\text{heater}}$ ) is 0.1 and the ambient view factor ( $F_{\text{am}}$ ) is 0.9.

In the case of the infrared sauna, infrared heating gives rise to energy transfer to the eye exposed to the sauna. In Figure 7, the effect of heater temperature is also investigated. This figure shows a comparison of temperature distribution within the eye at 10 min with a room air temperature of 80°C corresponding to heater temperatures of 200, 250, and 300°C. It is found that the heater temperature has a

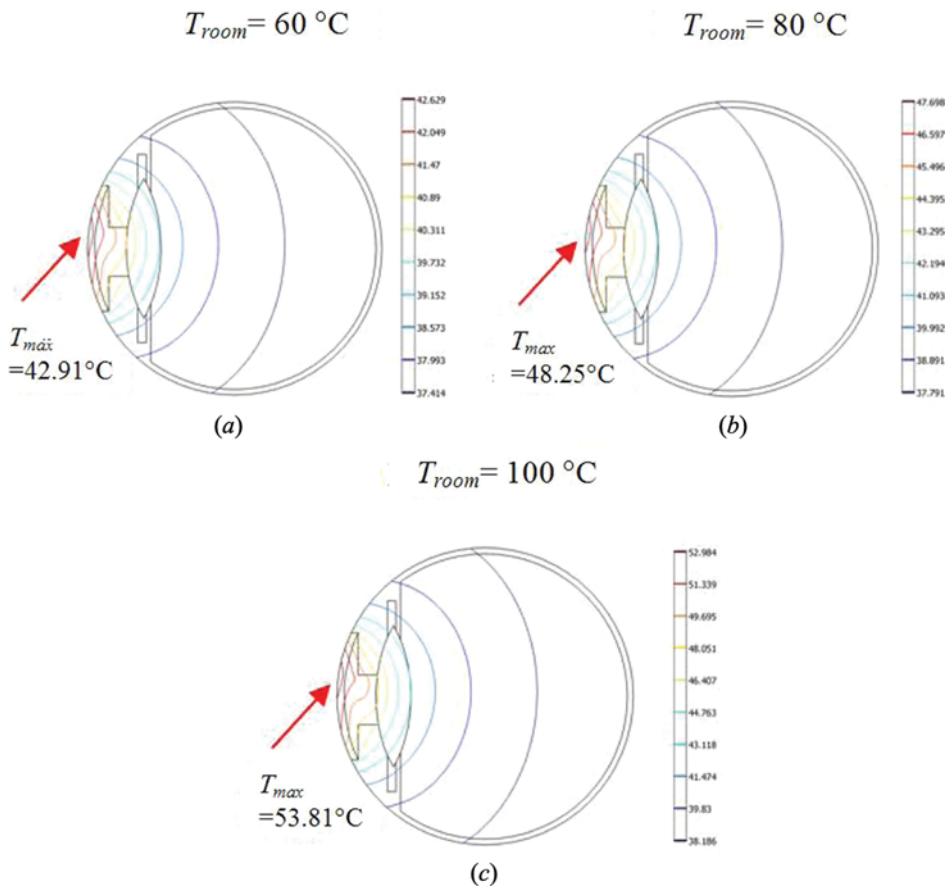


**Figure 6.** Temperature distribution in the eye exposed to a conventional sauna at room air temperatures of (a) 60°C, (b) 80°C, and (c) 100°C (at  $t = 10$  min).

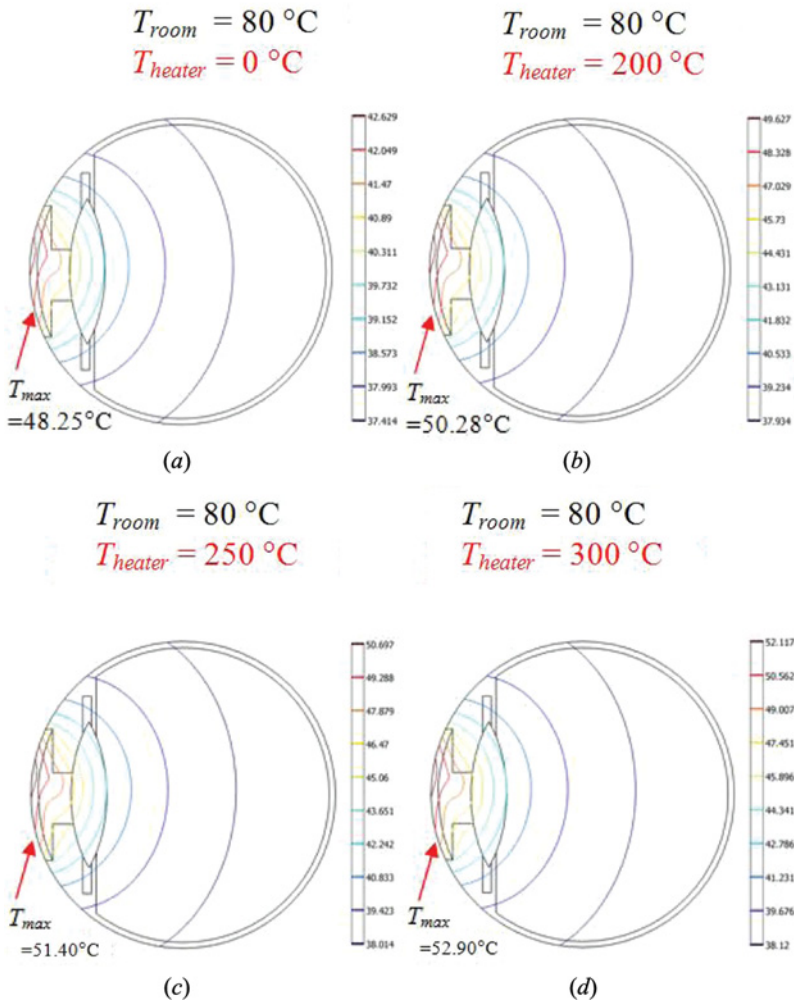


**Figure 7.** Temperature distribution in the eye exposed to an infrared sauna at a room air temperature of  $80\text{ }^{\circ}\text{C}$  and heater temperature set to (a) no heater, (b)  $200\text{ }^{\circ}\text{C}$ , (c)  $250\text{ }^{\circ}\text{C}$ , and (d)  $300\text{ }^{\circ}\text{C}$  (at  $t = 10\text{ min}$ ).

significant influence on temperature increase within the eye. Greater heater temperature provides greater heat radiation to the eye, thereby increasing the ocular temperature. During infrared sauna exposure at  $T_{room} = 80\text{ }^{\circ}\text{C}$ , the maximum temperatures in the eye are  $50.28$ ,  $51.40$ , and  $52.90\text{ }^{\circ}\text{C}$  for heater temperatures of  $200$ ,  $250$ , and  $300\text{ }^{\circ}\text{C}$ , respectively.

#### 4.4. Comparison Between Conventional and Infrared Sauna

Consider the temperature distribution at the extrusion line (Figure 8). Figure 9 shows the temperature distribution versus papillary axis (along the extrusion line) of

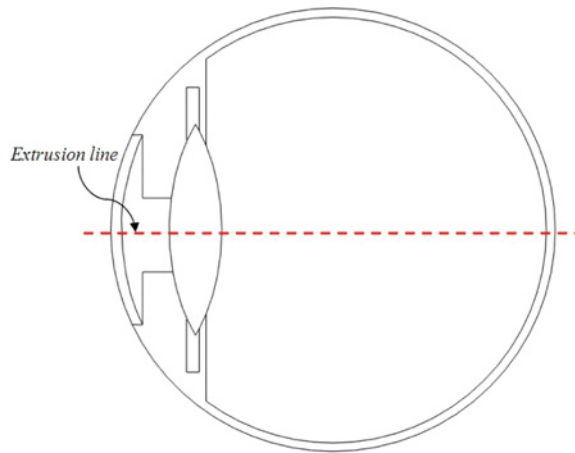


**Figure 8.** Extrusion line through the eye when temperature distribution is considered.

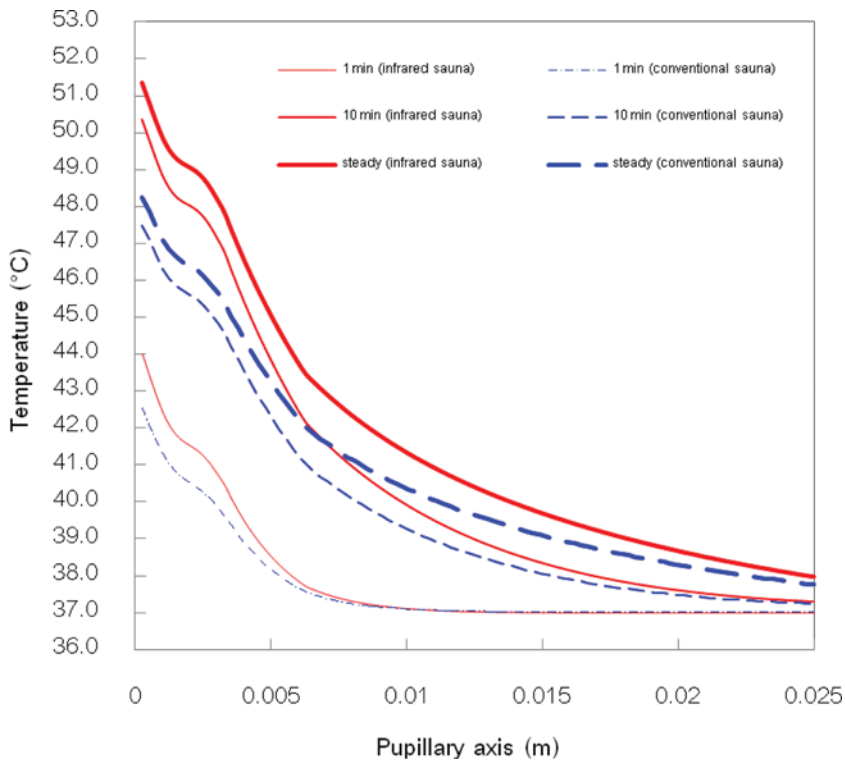


**Figure 9.** Temperature distribution versus papillary axis of the eye exposed to conventional and infrared sauna at various times.

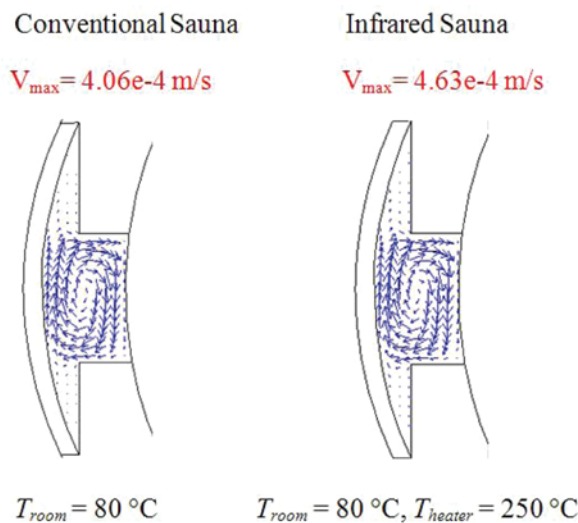
the eye exposed to conventional and infrared saunas at various times. This figure shows that the effect of sauna type has a substantial impact on temperature distribution within the eye for all exposure times. In all cases, the maximum temperature occurs at the corneal surface. At all exposure times, the infrared sauna induced a significantly higher temperature increase in the eye than did the conventional sauna.

Figure 10 shows the circulatory patterns within the anterior chamber exposed to conventional and infrared saunas at a room air temperature of  $80^{\circ}\text{C}$  and a heater temperature of  $250^{\circ}\text{C}$ . In both cases, a clockwise circulation appeared in the anterior chamber. This seems to imply that the heat gradually travels inward and passes through the front of the eye (cornea) to the lens.

In comparison, in the conventional case, the circulatory pattern has a lower speed than that of the infrared sauna. At low flow speed, the temperature gradient is less steep in the anterior chamber, where conduction is the dominant heat transfer mode across the fluid layer. On the other hand, in the case of the infrared sauna with higher flow speeds, different flow regimes are encountered with progressively increasing heat transfer. In this case, convective heat transfer plays a significant role in transferring heat.

The maximum velocities inside the anterior chamber are  $4.06 \times 10^{-4}$  and  $4.63 \times 10^{-4}$  m/s for the conventional and infrared sauna, respectively. Based on this study, it can be concluded that flow speed varies according to ocular temperature gradient.

In this study, the maximum temperature in the eye exposed to conventional and infrared sauna at  $T_{\text{heater}} = 300^{\circ}\text{C}$  for a room air temperature of  $80^{\circ}\text{C}$  is  $48.25$  and  $52.90^{\circ}\text{C}$ , respectively. This may cause potentially serious eye damage, especially in the case of exposure to the infrared sauna. The accumulated heat due to the combination of infrared energy and ambient air raises the eye temperature to  $52.90^{\circ}\text{C}$ ;



**Figure 10.** Velocity distribution inside the anterior chamber exposed to conventional and infrared sauna at a room air temperature of  $80^{\circ}\text{C}$  and a heater temperature of  $250^{\circ}\text{C}$ .

such a high temperature in the regions of the cornea and lens may lead to damaged eyesight and tissue destruction [2, 3].

## 5. CONCLUSIONS

While all saunas produce sweating, weight loss, detoxification of the body, and improved blood circulation, conventional saunas and infrared saunas do this differently. A conventional sauna warms the air, while an infrared sauna warms the objects in the air (i.e., a human within an enclosed space). This study focuses attention on the different heat transfer characteristics of conventional and infrared saunas. The effects of room air temperature and heater temperature on temperature distribution and fluid flow in the eye during exposure to sauna are systematically investigated. Temperature distribution in various ocular tissues during exposure is obtained by numerical simulation of a heat transfer model, which is then developed based on porous media theories.

It is found that increasing ocular temperature results from an increase in both room air temperature and heater temperature. The results show important information related to a complex interaction among ambient temperature, heater temperature, fluid flow, and temperature distribution in the eye during exposure to sauna. This study also shows that exposure time has a marked influence on temperature increase and fluid flow in the eye. At all exposure times, the infrared sauna induced a significantly higher ocular temperature increase than did the conventional sauna. Based on these results, saunas are potentially harmful to both eye and eyesight, especially the infrared sauna. Excessive or prolonged exposure to infrared sauna carries a higher risk of eye injury than conventional sauna. Staying within recommended time limits and wearing eye protection can help avoid risk.

The results obtained represent the phenomenon sufficiently accurately to determine the ocular temperature increase and enable recommendation of a guideline to indicate the limitations that must be considered at high temperatures due to sauna exposure under different conditions. Thus, the health effect assessment of sauna exposure requires the utilization of the most accurate numerical simulation of the thermal model. A further study will be developed to provide a more realistic 3D model for simulations. This will allow a better understanding of a realistic situation of the heat transfer process during sauna therapy.

## FUNDING

This work was financially supported by the Thailand Research Fund (TRF), the Commission on Higher Education (CHE), and Eastern Asia University.

## REFERENCES

1. R. D. Freeman and I. Fatt, Environmental Influences on Ocular Temperature, *Invest. Ophthalmol.*, vol. 12, no. 8, pp. 596–602, 1973.
2. A. F. Emery, P. Kramar, A. W. Guy, and J. C. Lin, Microwave Induced Temperature Rises in Rabbit Eyes in Cataract Research, *J. Heat Transfer ASME*, vol. 97, pp. 123–128, 1975.

3. C. Buccella, V. D. Santis, and M. Feliaiani, Prediction of Temperature Increase in Human Eyes Due to RF Sources, *IEEE Trans. Electromagn. Compat.*, vol. 49, no. 4, pp. 825–833, 2007.
4. J. C. Lin, Cataracts and Cell-Phone Radiation, *IEEE Antennas Propag. Mag.*, vol. 45, no. 1, pp. 171–174, 2003.
5. J. J. W. Lagendijk, A Mathematical Model to Calculate Temperature Distribution in Human and Rabbit Eye During Hyperthermic Treatment, *Phys. Med. Biol.*, vol. 27, pp. 1301–1311, 1982.
6. J. Scott, A Finite Element Model of Heat Transport in the Human Eye, *Phys. Med. Biol.*, vol. 33, pp. 227–241, 1988.
7. T. Wu, P. Li, Q. Shao, J. Hong, L. Yang, and S. Wu, A Simulation-Experiment Method to Characterize the Heat Transfer in Ex-Vivo Porcine Hepatic Tissue with a Realistic Microwave Ablation System, *Numer. Heat Transfer, Part A*, vol. 64, pp. 729–743, 2013.
8. E. H. Amara, Numerical Investigations on Thermal Effects of Laser–Ocular Media Interaction, *Int. J. Heat Mass Transfer*, vol. 38, pp. 2479–2488, 1995.
9. A. Hirata, S. Matsuyama, and T. Shiozawa, Temperature Rises in the Human Eye Exposed to EM Waves in the Frequency Range 0.6–6 GHz, *IEEE Trans. Electromagn. Compat.*, vol. 42, no. 4, pp. 386–393, 2000.
10. K. J. Chua, J. C. Ho, S. K. Chou, and M. R. Islam, On the Study of the Temperature Distribution within a Human Eye Subjected to a Laser Source, *Int. Commun. Heat Mass Transfer*, vol. 32, pp. 1057–1065, 2005.
11. W. Limtrakarn, S. Reepolmaha, and P. Dechaumphai, Transient Temperature Distribution on the Corneal Endothelium during Ophthalmic Phacoemulsification: a Numerical Simulation Using the Nodeless Variable Element, *Asian Biomed.*, vol. 4, no. 6, pp. 885–892, 2010.
12. S. Kumar, S. Acharya, R. Beuerman, and A. Palkama, Numerical Solution of Ocular Fluid Dynamics in a Rabbit Eye: Parametric Effects, *Ann. Biomed. Eng.*, vol. 34, pp. 530–544, 2006.
13. E. Ooi and E. Y. K. Ng, Simulation of Aqueous Humor Hydrodynamics in Human Eye Heat Transfer, *Comput. Biol. Med.*, vol. 38, pp. 252–262, 2008.
14. E. H. Ooi and E. Y. K. Ng, Effects of Natural Convection Inside the Anterior Chamber, *Int. J. Numer. Methods Biomed. Eng.*, vol. 27, pp. 408–423, 2011.
15. H. H. Pennes, Analysis of Tissue and Arterial Blood Temperatures in the Resting Human Forearm, *J. Appl. Physiol.*, vol. 1, pp. 93–122, 1948.
16. H. H. Pennes, Analysis of Tissue and Arterial Blood Temperatures in the Resting Human Forearm, *J. Appl. Physiol.*, vol. 85, no. 1, pp. 5–34, 1998.
17. V. M. M. Flyckt, B. W. Raaymakers, and J. J. W. Lagendijk, Modeling the Impact of Blood Flow on the Temperature Distribution in the Human Eye and the Orbit: Fixed Heat Transfer Coefficients Versus the Pennes Bioheat Model Versus Discrete Blood Vessels, *Phys. Med. Biol.*, vol. 51, pp. 5007–5021, 2006.
18. E. Y. K. Ng and E. H. Ooi, FEM Simulation of the Eye Structure with Bioheat Analysis, *Comput. Methods Program Biomed.*, vol. 82, pp. 268–276, 2006.
19. E. H. Ooi and E. Y. K. Ng, Ocular Temperature Distribution: A Mathematical Perspective, *J. Mech. Med. Biol.*, vol. 9, pp. 199–227, 2009.
20. A. Nakayama and F. Kuwahara, A General Bioheat Transfer Model Based on the Theory of Porous Media, *Int. J. Heat Mass Transfer*, vol. 51, pp. 3190–3199, 2008.
21. P. Rattanadecho, S. Suttisong, and T. Somtawin, The Numerical and Experimental Analysis of Heat Transport and Water Infiltration in a Granular Packed Bed Due to Supplied Hot Water, *Numer. Heat Transfer, Part A*, vol. 65, pp. 1007–1022, 2014.
22. K. Khanafer and K. Vafai, Synthesis of Mathematical Models Representing Bioheat Transport, *Adv. Numer. Heat Transfer*, vol. 3, pp. 1–28, 2009.

23. M. Shafahi and K. Vafai, Human Eye Response to Thermal Disturbances, *ASME J. Heat Transfer*, vol. 133, p. 011009, 2011.
24. J. Scott, The Computation of Temperature Rises in the Human Eye Induced by Infrared Radiation, *Phys. Med. Biol.*, vol. 33, pp. 243–257, 1988.
25. E. H. Amara, Numerical Investigations on Thermal Effects of Laser–Ocular Media Interaction, *Int. J. Heat Mass Transfer*, vol. 38, pp. 2479–2488, 1995.
26. A. Hirata, S. Matsuyama, and T. Shiozawa, Temperature Rises in the Human Eye Exposed to EM Waves in the Frequency Range 0.6–6 GHz, *IEEE Trans. Electromagn. Compat.*, vol. 42, no. 4, pp. 386–393, 2000.
27. K. J. Chua, J. C. Ho, S. K. Chou, and M. R. Islam, On the Study of the Temperature Distribution within a Human Eye Subjected to a Laser Source, *Int. Commun. Heat Mass Transfer*, vol. 32, pp. 1057–1065, 2005.
28. W. Limtrakarn, S. Reepolmaha, and P. Dechaumphai, Transient Temperature Distribution on the Corneal Endothelium during Ophthalmic Phacoemulsification: a Numerical Simulation Using the Nodeless Variable Element, *Asian Biomed.*, vol. 4, no. 6, pp. 885–892, 2010.
29. E. Y. K. Ng, J. H. Tan, U. R. Acharya, and J. S. Suri, *Human Eye Imaging and Modeling*, CRC Press, Florida, 2012. ISBN: 978-1-4398-6993-2.
30. D. Sumeet, U. R. Acharya, and E. Y. K. Ng, *Computational Analysis of Human Eye with Application*, WSPC Press, Singapore, 2011. ISBN: 978-981-4340-29-8.
31. E. Y. K. Ng, U. R. Acharya, J. S. Suri, and A. Campilho, *Image Analysis and Modeling in Ophthalmology*, CRC Press, Boca Raton, FL, 2014. ISBN: 978-1-4665-5930-1.
32. E. Y. K. Ng, U. R. Acharya, R. M. Rangayyan, and J. S. Suri, *Ophthalmology Imaging and Applications*, CRC Press, Florida, 2014.
33. E. H. Ooi, W. T. Ang, and E. Y. K. Ng, A Boundary Element Model of the Human Eye Undergoing Laser Thermokeratoplasty, *Comput. Biol. Med.*, vol. 28, pp. 727–738, 2008.
34. E. H. Ooi, W. T. Ang, and E. Y. K. Ng, A Boundary Element Model for Investigating the Effects of Eye Tumor on the Temperature Distribution inside the Human Eye, *Comput. Biol. Med.*, vol. 28, pp. 727–738, 2009.
35. J. H. Tan, E. Y. K. Ng, U. R. Acharya, and C. Chee, Study of Normal Ocular Thermogram Using Textural Parameters, *Infrared Phys. Technol.*, vol. 53, pp. 120–126, 2010.
36. J. H. Tan, E. Y. K. Ng, and U. R. Acharya, Evaluation of Tear Evaporation from Ocular Surface by Functional Infrared Thermography, *Med. Physics*, vol. 37, pp. 6022–6034, 2010.
37. J. H. Tan, E. Y. K. Ng, and U. R. Acharya, Evaluation of Topographical Variation in Ocular Surface Temperature by Functional Infrared Thermography, *Infrared Phys. Technol.*, vol. 54, pp. 469–477, 2011.
38. T. Wessapan, S. Srisawatdhisukul, and P. Rattanadecho, Numerical Analysis of Specific Absorption Rate and Heat Transfer in the Human Body Exposed to Leakage Electromagnetic Field at 915 MHz and 2450 MHz, *ASME J. Heat Transfer*, vol. 133, p. 051101, 2011.
39. T. Wessapan, S. Srisawatdhisukul, and P. Rattanadecho, The Effects of Dielectric Shield on Specific Absorption Rate and Heat Transfer in the Human Body Exposed to Leakage Microwave Energy, *Int. Commun. Heat Mass Transfer*, vol. 38, pp. 255–262, 2011.
40. T. Wessapan and P. Rattanadecho, Numerical Analysis of Specific Absorption Rate and Heat Transfer in Human Head Subjected to Mobile Phone Radiation, *ASME J. Heat Transfer*, vol. 134, p. 121101, 2012.
41. T. Wessapan, S. Srisawatdhisukul, and P. Rattanadecho, Specific Absorption Rate and Temperature Distributions in Human Head Subjected to Mobile Phone Radiation at Different Frequencies, *Int. J. Heat Mass Transfer*, vol. 55, pp. 347–359, 2012.

42. P. Keangin, T. Wessapan, and P. Rattanadecho, Analysis of Heat Transfer in Deformed Liver Cancer Modeling Treated Using a Microwave Coaxial Antenna, *Appl. Therm. Eng.*, vol. 31, no. 16, pp. 3243–3254, 2011.
43. P. Keangin, T. Wessapan, and P. Rattanadecho, An Analysis of Heat Transfer in Liver Tissue during Microwave Ablation Using Single and Double Slot Antenna, *Int. Commun. Heat Mass Transfer*, vol. 38, pp. 757–766, 2011.
44. P. Rattanadecho and P. Keangin, Numerical Study of Heat Transfer and Blood Flow in Two-Layered Porous Liver Tissue During Microwave Ablation Process Using Single and Double Slot Antenna, *Int. J. Heat Mass Transfer*, vol. 58, pp. 457–470, 2013.
45. T. Wessapan and P. Rattanadecho, Specific Absorption Rate and Temperature Increase in Human Eye Subjected to Electromagnetic Fields at 900 MHz, *ASME J. Heat Transfer*, vol. 134, p. 091101, 2012.
46. T. Wessapan and P. Rattanadecho, Specific Absorption Rate and Temperature Increase in the Human Eye due to Electromagnetic Fields Exposure at Different Frequencies, *Int. J. Heat Mass Transfer*, vol. 64, pp. 426–435, 2013.
47. T. Wessapan and P. Rattanadecho, Influence of Ambient Temperature on Heat Transfer in the Human Eye during Exposure to Electromagnetic Fields at 900 MHz, *Int. J. Heat Mass Transfer*, vol. 70, pp. 378–388, 2014.